

## DYNAMIC BEHAVIOR OF GAS-SOLID FLOW IN HORIZONTAL PIPES

Dr. Khailed Abd Al Hameed  
Univ. of Technology  
Dept. of Mech. Eng.

Dr. Tahseen Al-Hattab  
Univ. of Babylon  
Dept. of Electrochem. Eng.

Dr. Riyadh Al-Turhee  
Univ. of Babylon  
Dept. of Mech. Eng.

### ABSTRACT

The dynamic behavior of a two phase (gas-solid) flow in a horizontal pipe is studied in this work. The experimental and theoretical methods are set to examine the effects of inlet velocity, loading ratio for different sizes of solid particles on the pressure, velocity and the volume phase fraction along the pipe. The range of velocities used in this work are between (12-42 m/s) and the loading ratios are between (2-12) as mass of solid to mass of air. The solid is the sand at four groups of particle size ( $150-300 \mu m$ ), ( $300-425 \mu m$ ), ( $425-600 \mu m$ ) and ( $600-850 \mu m$ ). The experimental rig is constructed to measure the inlet velocity and pressure along (3.175cm) diameter (6m) long horizontal pipe. The results show that the loading ratio (LR) and Reynolds number (Re) are the main parameters that control the pressure drop along the pipe. The pressure drop increases as both Reynolds number and loading ratio increase whereas the effect of particle size is opposite to that effect. The pressure drop for a small particle is less than for the larger one. The empirical correlation that relates the friction coefficient (Cf) through the pipe is represented by the dimensionless groups (Re), (volume fraction,  $\alpha$ ) and (Froude number, Fr).

$$C_{f \text{ exp}} = 9.737 \cdot \alpha^{-1.356} Re^{-0.809} Fr^{0.125}$$

The theoretical analysis consists of the solution of the steady state and the unsteady state of the differential equations using the boundary conditions that govern the two phase (gas-solid) flow GSVF is the computer program that was build to simulate the dynamic behavior of the flow involved in the semi-empirical correlation for (gas-solid) interaction (Sa). The dimensionless number (SR) suggested in this work indicates that the volume fraction is the most effective parameter than Re and Fr.

$$S_R = 5.3 \times 10^{-3} \alpha^{0.848} Re^{-0.004} Fr^{0.008}$$

The volume fraction, velocity and pressure profiles are evaluated as the output of the computer program, only the pressure profiles are compared with the experimental values. The pressure drop and the friction coefficients produced from the theoretical analysis show that the theoretical values are (24%) higher than the experimental one.

$$C_{f \text{ theo.}} = 7.207 \alpha^{-1.368} Re^{-0.681} Fr^{0.077}$$

### الخلاصة

في هذا العمل تمت دراسة التصرف الديناميكي للجريان ثنائي الطور في الأنابيب الأفقية. تمت دراسة العملية والنظرية على أساس تأثير كل من سرعة الدخول ونسبة التحميل لمختلف أحجام الجزيئات الصلبة على كل من الضغط والسرعة و نسبة التحميل ( $\alpha$ ). إن معدل السرعة المستخدمة في هذا العمل تتراوح بين (2-12) م/ثا و نسب التحميل بين (2-12) كنسبة المادة الصلبة إلى الهواء. وأحجام الأجسام الصلبة (الرمل) المستخدمة هي أربع أحجام كالآتي ( $150-300 \mu m$ )، ( $300-425 \mu m$ )، ( $425-600 \mu m$ ) و ( $600-850 \mu m$ ). تم بناء جهاز مختبري لقياس سرعة الدخول والضغط لأنبوب أفقي قطره (3.175 سم) وطول (6 م). النتائج تبين إن نسبة التحميل (LR) ورقم رينولدز (Re) هي العوامل الرئيسية التي تسيطر على هبوط الضغط على طول الأنبوب و أن انخفاض الضغط يزداد بزيادة كل من نسبة التحميل ورقم رينولدز،

بينما تكون الصورة معكوسة بالنسبة لحجم الجزيئات الصلبة حيث يكون الانخفاض كبير بالنسبة للجزيئات الصغيرة أكثر من الجزيئات الكبيرة. في هذا العمل تم تقديم علاقة تجريبية ل (Cf) خلال الأنبوب ترتبط بمجموعة لا بعدية من (  $\alpha$  , Fr , Re )

$$C_{fExp} = 9.737 \cdot \alpha^{-1.356} Re^{-.809} Fr^{0.125}$$

التحليل النظري يتضمن حل للحالة المستقرة والحالة غير مستقرة للمعادلات التفاضلية والشروط الحدية التي تتضمن الجريان الثنائي الطور (غازي-صلب). تم بناء برنامج (GSVF) لتخمين التصرف الديناميكي للجريان يتضمن علاقات شبه تجريبية (للغاز والصلب) ل (Sa) و الرقم اللابعدي (SR) الذي اقترح في هذا العمل ليعطينا تصور أن (  $\alpha$  ) هي أكثر العوامل تأثيراً على الجريان أكثر من (Re) و (Fr) .

$$S_R = 5.3 \times 10^{-3} \alpha^{0.848} Re^{-0.004} Fr^{0.008}$$

تم إيجاد كل من (U, P,  $\alpha$ ) كنواتج من البرنامج ، الضغط فقط تمت مقارنته مع القيم العملية . ان فرق الضغط و (  $\alpha$  ) المحسوبة من التحليل النظري تبين أن القيم النظرية أكثر ب(24%) من النتائج العملية.

$$C_{f\ theo.} = 7.207 \alpha^{-1.368} Re^{-0.681} Fr^{0.077}$$

## INTRODUCTION

The flow in pipe is one of the simplest and best understood flow configuration in the area of the two phase flow studies and numerous experimental ,theoretical and numerical investigation are available.

The pneumatic conveying of particles in pipes or channels is one of the most important technological process in industry and hence many publications are available in this area, However, (SHIMIZU et al 1978) presented an experimental study on the flow characteristics of a dilute gas-solid suspension medium in a circular tube, where in the inlet entry length and the fractional pressure-drop were measured systematically. In particular, the effects of particle size on the fractional pressure-drop are presented in some detail. (YUTAKA TSUJI and YOSHINOBU MORIKAWA 1982), made an experiment on an air-solid two-phase flow in a horizontal pipe. The main concern was the relation between flow patterns and pressure fluctuation at low air velocities. First, the flow patterns were classified into five different types depending on the air and particle flow rates. Next, it was shown how the properties of pressure fluctuation change as the air velocity decreases. Further, they analyzed the fluctuation signals in detail and discussed differences due to the flow patterns and particle size. (HAMED and MOHAMED 2001), conducted an experimental investigation to simultaneously measure the instantaneous velocities of large particle and air in a two-phase flow using laser Doppler velocimeter. They used measurements at two photo-Multiplier voltage settings to separate the signals from the small seeding particles that trace the air flow and the suspended solid particle based on the difference of scattered light intensity. (MASAHIRO TAKEI et al 2002), launched a concept to extract a feature of solid-air two-phase flow in a pipeline with a combination of a capacitance-computed tomography and wavelets transform.

With this concept, they obtained particle distribution images by CT transform with discrete wavelets multi resolution. As a result, in the case of low open area ratios of the pipe cross-section, high particle densities were shown in secondary dominant levels as well as a substantial space level. The high value in the secondary level resulted from inhomogeneous density due to collision between particles. (HAMED and MOHAMED 2001), conducted an experimental investigation to simultaneously measure the instantaneous velocities of large particle and air in a two-phase flow

using laser Doppler velocimeter. They used measurements at two photo-Multiplier voltage settings to separate the signals from the small seeding particles that trace the air flow and the suspended solid particle based on the difference of scattered light intensity. (MASAHIRO TAKEI et al 2002), launched a concept to extract a feature of solid-air two-phase flow in a pipeline with a combination of a capacitance-computed tomography and wavelets transform. With this concept, they obtained particle distribution images by CT transform with discrete wavelets multi resolution. As a result, in the case of low open area ratios of the pipe cross-section, high particle densities were shown in secondary dominant levels as well as a substantial space level. The high value in the secondary level resulted from inhomogeneous density due to collision between particles. (YANG NING et al 2003), had extensively corroborated Meso-scale structure existing in the form of particle clusters or strands in concurrent-up gas-solid two-phase flow in experimental research. However, it was significant effects on interfacial drag coefficient are seldom taken into account in current Computational Fluid Dynamic (CFD) simulations by using the two-fluid models. They described the Energy-Minimization Multi-Scale (EMMS) approach, in which the heterogeneous structure by the so-called multi-scale resolution and energy-minimization method, was adapted for investigating the dependence of drag coefficient on structure parameters. The calculated structure-dependent drag coefficients from the EMMS approach were then incorporated into the two-fluid model to simulate the behavior of the concurrent-up gas-solid flow in a riser.

## THE MATHEMATICAL MODEL

### Governing Equations

The governing equations represent the continuity and the momentum equation in gas-solid phase are considered below with the assumption of one dimensional unsteady state flow.

For gas phase

$$\begin{aligned} \frac{\partial \alpha_a}{\partial t} + U \frac{\partial \alpha_a}{\partial x} &= S_a \\ \frac{\partial (\alpha_a \rho_a)}{\partial t} + \frac{\partial (\alpha_a \rho_a U)}{\partial x} &= 0 \\ \frac{\partial (\alpha_a \rho_a U)}{\partial t} + \frac{\partial (\alpha_a \rho_a U^2 + \alpha_a p)}{\partial x} &= +P \frac{\partial \alpha_a}{\partial x} + M \end{aligned}$$

For solid phase

$$\begin{aligned} \frac{\partial (\alpha_b \rho_b)}{\partial t} + \frac{\partial (\alpha_b \rho_b U)}{\partial x} &= 0 \\ \frac{\partial (\alpha_b \rho_b U)}{\partial t} + \frac{\partial (\alpha_b \rho_b U^2 + \alpha_b p)}{\partial x} &= -P \frac{\partial \alpha_a}{\partial x} - M \end{aligned} \tag{1}$$

$$\alpha_a + \alpha_b = 1$$

Where  $(\alpha, U, \rho, p)$  are the phase fraction, the mass average velocity, density and the pressure respectively, whereas  $(P, M, S_a)$  are the model parameters which can be obtained experimentally.

However, in order to overcome some difficulties in determination of system parameters, the corresponding momentum single-phase equations are summed to result in the following set of equations:

$$\begin{aligned}
\frac{\partial \alpha_a}{\partial t} + U \frac{\partial \alpha_a}{\partial x} &= S_a \\
\frac{\partial(\alpha_a \rho_a)}{\partial t} + \frac{\partial(\alpha_a \rho_a U)}{\partial x} &= 0 \\
\frac{\partial(\alpha_b \rho_b)}{\partial t} + \frac{\partial(\alpha_b \rho_b U)}{\partial x} &= 0 \\
\frac{\partial((\alpha_a \rho_a + \alpha_b \rho_b)U)}{\partial t} + \frac{\partial((\alpha_a \rho_a + \alpha_b \rho_b)U^2 + p)}{\partial x} &= 0
\end{aligned} \tag{2}$$

Notice that ( $S_a$ ), solid-gas interaction factor, is only the single parameter which needed to be determined from experimental data

### STEADY STATE SOLUTION

In order to evaluate the system parameter ( $S_a$ ), the steady state solution is used to analyze the experimental data and determine its value as a function of different values of operation variables. Taking into account that:

$$\alpha_b = 1 - \alpha_a$$

$$\rho_a = \frac{p}{RT}$$

$$\frac{\partial \rho_b}{\partial x} = 0, \quad \text{constant solid density}$$

At the steady state the system of equation (3-2) reduces to the following set of equations:

$$\begin{aligned}
U \frac{\partial \alpha}{\partial x} &= S_a \\
\frac{\partial(\alpha \rho_a U)}{\partial x} &= 0 \\
\frac{\partial((\alpha_a \rho_a + \alpha_b \rho_b)U^2 + p)}{\partial x} &= 0
\end{aligned} \tag{3}$$

(hereafter we denote  $(\alpha_a, \rho_a)$  as  $(\alpha, \rho)$  respectively).

At the steady state, we are assumed that the approximate profiles of velocity, pressure and phase fraction are as follows :

$$\begin{aligned}
U &= U_o e^{-\lambda x} \\
p &= p_o e^{-\mu x} \\
\alpha &= \alpha_o e^{-\gamma x}
\end{aligned} \tag{4}$$

Where  $(\alpha_o, U_o, p_o)$  are the values of each variable at  $x=0$ , and the constants  $(\lambda, \gamma, \mu)$  are still unknown which can be evaluated later.

Substitution of equations (4) into equations (3) results the following set of equation:

$$\begin{aligned}
 U_o \alpha_o \gamma e^{-(\lambda+\gamma)x} &= -S_a \\
 \alpha_o \frac{P_o}{RT} (-\lambda U) e^{-(\gamma+\mu+\lambda)x} + \left( \frac{-P_o}{RT} U_o \gamma \alpha_o \right) e^{-(\gamma+\mu+\lambda)x} + \left( \alpha_o U_o \left( \frac{P_o}{RT} \right) \right) (-\mu) e^{-(\gamma+\mu+\lambda)x} &= 0 \\
 \left[ \frac{P_o}{RT} e^{-\mu x} (-\gamma \alpha_o e^{-\gamma x}) + \alpha_o e^{-\gamma x} \left( \frac{P_o}{RT} \right) (-\mu) e^{-\mu x} + \gamma \rho_b \alpha_o e^{-\gamma x} \right] \cdot U_o^2 e^{-2\lambda x} \\
 + 2U_o e^{-\lambda x} (-\lambda) U_o e^{-\lambda x} \left( \alpha_o e^{-\gamma x} \left( \frac{P_o}{RT} \right) e^{-\mu x} + \rho_b - \alpha_o e^{-\gamma x} \rho_b \right) + p_o (-\mu) e^{-\mu x} &= 0
 \end{aligned} \tag{5}$$

After some simplification, the above equations are reduced :

$$\begin{aligned}
 \lambda + \gamma - \ln \left( \frac{U_o \alpha_o \gamma}{-S_a} \right) &= 0 \\
 \gamma + \mu + \lambda &= 0 \\
 \gamma \left( \frac{\rho_b}{\rho_o} - 1 \right) - \mu \left( 1 + \frac{P_o}{\alpha_o \rho_o U_o^2} \right) - 2\lambda \left( 1 + \left( \frac{1}{\alpha_o} - 1 \right) \frac{\rho_b}{\rho_o} \right) &= 0
 \end{aligned} \tag{6}$$

where  $\rho_o = \frac{P_o}{RT}$

It is clear that the unknown constants ( $\lambda, \gamma, \mu$ ) can not be evaluated before the determination of system parameter ( $S_a$ ). Therefore we suggest a numerical procedure that can solve the problem and determine the unknown parameters. The procedure is basically dependant on the so called (Least Square Method) for minimization of errors between the approximated (theoretical) profile of pressure and the measured values of pressure at the steady state conditions. The algorithm of this method is :

- Assume given value of ( $S_a$ ),
- Solve the system of equations (6) to determine  $\psi = f(S_a, \gamma, \mu, \lambda)$  for specified operation variables.

- Evaluate the approximate pressure profile

$$P_{theo} = p_o e^{-\mu x}$$

- Evaluate the errors ,(refer to Fig.(1)), between the theoretical ( $P_{theo}$ ) and the experimental ( $P_{exp.}$ ) pressure profiles according to the following equation:

$$Minimum \ Errors = \sum_{i=1}^N (P_{theo.} - P_{exp.})^2 \tag{7}$$

### UNSTEADY STATE SOLUTION

The transient behavior of solid-gas flow can be predicted using the values of ( $S_a$ ), evaluated in the previous section .

A finite difference method is used to discretize the system of differential equation (2). The iterative method is used to solve the resulting equations. However, the following steps summarize the procedure used :

$$\begin{aligned} \frac{\partial \alpha}{\partial t} &= S_a - U \frac{\partial \alpha}{\partial x} \\ \frac{\partial p}{\partial t} &= - \left( p \frac{\partial U}{\partial x} + U \frac{\partial p}{\partial x} \right) - p \left( \frac{\partial \alpha}{\partial t} + U \frac{\partial \alpha}{\partial x} \right) / \alpha \\ \frac{\partial U}{\partial t} &= \left[ \begin{array}{l} - \left( \frac{p}{RT} \frac{\partial \alpha}{\partial t} + \frac{\alpha}{RT} \frac{\partial p}{\partial t} - \rho_b \frac{\partial \alpha}{\partial t} \right) U \\ - \left( \frac{\alpha}{RT} \frac{\partial p}{\partial x} + \frac{p}{RT} \frac{\partial \alpha}{\partial x} - \rho_b \frac{\partial \alpha}{\partial x} \right) U^2 \\ - 2U \left( \alpha \frac{p}{RT} + \rho_b (1 - \alpha) \right) \frac{\partial U}{\partial x} - \frac{\partial p}{\partial x} \end{array} \right] / \left( \alpha \frac{p}{RT} + \rho_b (1 - \alpha) \right) \end{aligned} \quad (8)$$

The explicit finite difference method and backward finite difference method were used to discretize the derivatives in time domain and space domain respectively, Fig.(2). When

$$A \equiv f(x, t) \Rightarrow A_x^t,$$

Where A is any variable from (p u .α)

then :

$$\text{the time derivative : } \frac{\partial A}{\partial t} = \frac{A_x^{t+\Delta t} - A_x^t}{\Delta t}$$

$$\text{and the space derivative : } \frac{\partial A}{\partial x} = \frac{A_x^t - A_{x-\Delta x}^t}{\Delta x}.$$

Apply the above expressions into the system of eq. (8), results in the following finite difference algebraic equations.

$$\begin{aligned} \frac{\partial y}{\partial t} &= \frac{\partial f}{\partial t} = \frac{f_A}{\Delta x} \\ \frac{f_A}{\Delta x} &= \frac{\partial A}{\partial t} = \frac{A_x^{t+\Delta t} - A_x^t}{\Delta t} \\ A_x^{t+\Delta t} &= A_x^t + \frac{\Delta t}{\Delta x} \cdot f_A \end{aligned} \quad (9)$$

where the functions ( $f_A$ ) can be written as follows :

$$\begin{pmatrix} f_\alpha \\ f_p \\ f_U \end{pmatrix} = \begin{bmatrix} C_{\alpha 0} & C_{\alpha 1} & C_{\alpha 2} & C_{\alpha 3} & C_{\alpha 4} & C_{\alpha 5} & C_{\alpha 6} \\ C_{p0} & C_{p1} & C_{p2} & C_{p3} & C_{p4} & C_{p5} & C_{p6} \\ C_{U0} & C_{U1} & C_{U2} & C_{U3} & C_{U4} & C_{U5} & C_{U6} \end{bmatrix} \cdot \begin{pmatrix} I \\ \alpha_x^t \\ \alpha_{x-\Delta x}^t \\ p_x^t \\ p_{x-\Delta x}^t \\ U_{xx}^t \\ U_{x-\Delta x}^t \end{pmatrix}$$

where :

$$C_{\alpha 0} = S_a \cdot \Delta x$$

$$C_{\alpha 1} = -U_x^t$$

$$C_{\alpha 2} = -C_{\alpha 1}$$

$$C_{\alpha 3} = C_{\alpha 4} = C_{\alpha 5} = C_{\alpha 6} = 0$$

$$C_{p0} = -S_a p_x^t \Delta x / \alpha_x^t$$

$$C_{p1} = -p_x^t U_x^t / \alpha_x^t + p_x^t U_x^t,$$

$$C_{p2} = -C_{p1}$$

$$C_{p3} = -U_x^t,$$

$$C_{p4} = -C_{p5}$$

$$C_{p5} = -p_x^t,$$

$$C_{p6} = -C_{p5}$$

$$C_{U0} = U_x^t S_a p_x^t \Delta x / RT + S_a \left( \frac{p_x^t}{RT} - \rho_b \right) \Delta x$$

$$C_{U1} = \begin{bmatrix} -U_x^t \left( \frac{p_x^t}{RT} - \rho_b \right) + p_x^t U_x^t / RT \\ -p_x^t U_x^t \alpha_x^t / RT + \left( \frac{p_x^t}{RT} - \rho_b \right) U_x^t \alpha_x^t \end{bmatrix}, \quad C_{U2} = -C_{U1}$$

$$C_{U3} = - \left( 1 + \frac{\alpha_x^t U_x^t}{RT} \right) + U_x^t \alpha_x^t / RT, \quad C_{U4} = -C_{U5}$$

$$C_{U5} = -2U_x^t \left( \frac{\alpha_x^t p_x^t}{RT} + (1 - \alpha_x^t) \rho_b \right) + U_x^t p_x^t / RT, \quad C_{U6} = -C_{U5}$$

▪ **Initial and Boundary Condition:**

The initial and boundary conditions used in this work are:

At  $t=0$  (initial conditions)

$$\alpha_x^0 = 1$$

$$\left. \begin{matrix} p_x^0 \\ U_x^0 \end{matrix} \right\} =$$

Are the solution of the steady state profile of isothermal air flow through the pipe governing by the following equations:

$$\rho_{x+\Delta x} U_{x+\Delta x} = \rho_x U_x \quad (10)$$

since

$$p_x^2 - p_{x+\Delta x}^2 = RT(\rho U)_{x+\Delta x/2}^2 \left( f \frac{L}{D} + 2 \ln \left( \frac{p_x}{p_{x+\Delta x}} \right) \right) \quad (11)$$

$$f = \frac{0.3164}{\text{Re}^{1/4}} \quad (12)$$

which needs another subroutine to evaluate the initial profiles numerically at the start of computations.

At  $x=0$  (boundary conditions)

$$\alpha_0^t = \alpha_o$$

$$p_0^t = p_o$$

$$U_0^t = U_o$$

#### ▪ **Solution:**

Direct iterative method is used to evaluate the profiles of  $(\alpha, p, U)$  at each time step with the following convergence criteria of the solution :

$$\sum_{k=1}^N \left| \left( \frac{A_k^{t+\Delta t}}{A_k^t} - 1 \right) \right| \leq \varepsilon \quad (13)$$

where (N) is the number of divisions in (x-domain). It is found that the best value of accuracy ( $\varepsilon$ ) is  $\approx 10^{-4}$  for (N=40). These values perform the more stable solutions.

#### ▪ **GSVF program**

Figure (3) shows the flow chart of the computer program used in this work. It is designed to study the transient behavior of Gas-Solid Visual Flow (GSVF).

The Visual Basic language is used to develop program as multi-input and multi-output variables. The results show the variations of determined variables  $(\alpha, U, p)$  at each time step. The profiles are represented as curves on the screen also they are saved as tabulated data in external files.

The program also includes a part for simulation of particles movement through the pipe. The simulation is based on random walk analysis which is used to expand the one dimension solution of transient profile to two dimension distribution of the particle at any time. The predicted images of particles movement through the pipe are saved in order to collect the images as a movie.

Fig.(4) shows a screen shot of GSVF program for certain values of operation parameters and some samples of images saved from the program after different time steps.

### The Experimental equipment

Fig.(5) shows the experimental equipments and measuring system. The experimental equipment includes the following:

Air compressor, Air storage tank, Air regulator, Orifice meter, Solid (sand) storage, tank and ball valve, Injection nozzle, Multi manometer, U- tube manometer, Main pipe, Cyclone Separator, Digital Camera, and Digital Balance.

### The Experimental Procedure :

One hundred and twenty experiment sets were conducted in this work in order to study and analyze the friction through the sand –air flow.

Each experiments was repeated three times to ensure confidence of the results. For each sand particle size the experimental procedure to determine pressure drop through the pipe ,consist of the following steps:

- 1- fill the hopper (sand storage tank) with a bout of (25 kg) of the selected mesh size of the sand .
- 2- Switch on the air compressor until the pressure inside the storage tank reaches the operating pressure ( a bout 2 bar)
- 3- Open the regulator valve to feed the air through the pipe. The pressure drop through the orifice is measured to determine the air velocity under steady state conditions.
- 4- Open the ball valve connected to the hopper of the sand .The opening gauge is proportional to the required loading ratio.
- 5- During this period we measured the pressure drop through each point of the pipe by recording the color water head in the multi-manometer.
- 6- Measure the weight of precipitate sand leaving the cyclone ,to determine the mass flow rate of the sand and the loading ratio of the two phases.

The steady state of the flow is considered when the pressure drop profile through the pipe is approximately steady

## RESULTS

### Experimental Results:

The influence of particle size input velocity and loading ratio are examined for more than 140 experiments with (2 or 3) time of repetitions. the pressure profile are almost nonlinear . Therefore it is better to evaluate the average pressure drop rather than the evaluation of the pressure drop based on linear assumption profile. Accordingly, the average pressure drop can be determined as follows :

$$\left(\frac{\Delta P}{L}\right) = \left(\frac{\overline{\Delta P}}{L}\right) = \left(\frac{\sum_{i=1}^N \left(\frac{\Delta P}{L}\right)_i}{N}\right) \quad (14)$$

Where N is the number of subsection that the pressure drop where measured along the test section. Here it is equal to ( 4 ) in this work.

### Effect of Loading Ratio ( $L_R$ ):

Figures (6) show the effect of loading ratio on the relationship between the pressure drop and Reynolds number for different values of particle sizes.

For a certain value of particle size the pressure drop along the test section of the pipe increases as Reynolds number and loading ratio increases. These relationships are similar in trend for every particle size used in this work.

Moreover, at low Reynolds number the effect of increasing loading ratio on the pressure drop is small compared with that at high Reynolds number. For particle size (300-425  $\mu\text{m}$ ), at Reynolds number ( $Re=23582$ ) the pressure drop increases from (147 Pa/m) to (588 Pa/m) when the loading ratio increases from (3.69) to (9.24). But at ( $Re=107142$ ) the pressure drop increases from (880 Pa/m) to (2260 Pa/m) for the same change in loading ratio.

In this work, an empirical correlation for the friction coefficient ( $C_f$ ) as a function of Reynolds number ( $Re$ ), the two phase volume fraction ( $\alpha$ ) and Froud number ( $Fr$ ) is proposed. The experimental values of the friction coefficient evaluated based on pressure drop are collected in a form of the following equations:

$$C_f = c \cdot \alpha^{n1} Re^{n2} Fr^{n3} \quad (15)$$

A computer program was used to determine the coefficients of the above equation. The dimensionless groups are evaluated at the same ranges of the experimental data in this work.

The final form of the ( $C_f$ ) correlation extracted from the experimental data is as follows :

$$C_f = 9.737 \cdot \alpha^{-1.356} Re^{-0.809} Fr^{0.125} \quad (16)$$

Figure (7) shows the comparison between the experimental data and the correlated values calculated according to equation(16). The figure shows that there is a good relation between the data, taken into consideration that the correlation factor is ( $R^2=0.933$ ).

However, the correlation indicates that the friction coefficient depend strongly on both ( $Re$ ) and ( $\alpha$ ) and there is less effect of ( $Fr$ ) on the ( $C_f$ ).

## Theoretical Results

### Correlations for ( $S_a$ ):

According to the suggested procedure and the computer program algorithm used by Andrianov, it have been evaluated more than (140) of different values of ( $S_a$ ) related to such variables. These values were correlated by functions into two different manners. The first correlation is as a direct relation between ( $S_a$ ) and the loading ratio ( $L_R$ ), inlet velocity ( $U$ ) and particle size ( $D_p$ ), shown as follows:

$$S_a = 0.146 L_R^{-0.664} U^{1.002} d_p^{-0.006} \quad (17)$$

Where  $S_a$  in ( $s^{-1}$ ),  $U$  in (m/s) and  $d_p$  in ( $\mu\text{m}$ ).

The second correlation that relates the values of ( $S_a$ ) and other parameters is a dimensionless group formula. The following formula is suggested here:

$$S_R = \left( S_a \cdot \frac{D}{U} \right) \approx f(\alpha, Re, Fr) \quad (18)$$

where ( $S_R$ ) is the suitable dimensionless group of ( $S_a$ ) which also combines the pipe diameter ( $D$ ) and the inlet velocity ( $U$ ) as a new dimensionless number appears in this field of knowledge. It may look-like the dimensionless number called as (Strouhal number,  $S_t$ ) which describes the oscillating flow mechanisms. Therefore this number will be the (key) to start and complete the theoretical analysis.

However the calculations according to the second formula results in the following expression :

$$S_R = 5.3 \times 10^{-3} \alpha^{0.848} Re^{-0.004} Fr^{0.008} \quad (19)$$

The comparison between the experimental data and the predicted formula (20), show an excellent accuracy that one cannot expect. The correlation coefficient slightly differs from unity ( $R^2=0.999$ ). According to both formula, one can conclude that the particle size has a little effect on the values ( $S_a$ ) or ( $S_R$ ) whereas the inlet velocity is affected by about (1.5) of that of the loading ratio. The effect of the two variables is at an inverse manner. Following the same way used in the experimental work the following correlation is extracted from the theoretical data which relate the friction coefficient with Reynolds number, volume fraction and Froud number.

$$C_{f \text{ theo.}} = 7.207 \alpha^{-1.368} Re^{-0.681} Fr^{0.077} \quad (20)$$

Figure (8) shows the comparison between the theoretical data and the correlated values calculated according to equation(20). According to formula (21), it is found that the theoretical friction coefficient is about (24%) higher than the experimental one.

$$\text{Average Difference} = \frac{1}{N} \left( \sum_{i=1}^N \left( \frac{C_{f \text{ theo.}}}{C_{f \text{ exp.}}} - 1 \right) \right) \cdot 100\% \quad (21)$$

Figs (9) to (11) show samples of the unsteady state solution of the  $(\alpha, U, p)$  for some values of  $(\alpha_o, U_o, p_o)$ . Whereas both  $(\alpha)$  and  $(U)$  profiles are still as predicted ones and there is no way to judge whether they are " True" or not as magnitudes except one believes that the trend of solution follows the essential solutions of the differential equations. It is shown that the  $(\alpha)$  profile behaves as a wave that moves from the origin of time-distance coordinates (0,0) in both directions toward the ends of the axis. It is also found that the speed of this wave depends on the system parameter  $(\alpha_o, U_o, P_o)$ . This behavior is mainly reflected on pressure profile especially in the first steps when the pressure decreases steeply to approximate steady state profile, which decreases with pipe distance. The velocity profile solution behaves at different matter in the first steps of time. It is to a maximum value all over the pipe after some steps of time then the velocity decreases to reach the steady state profile. Figure (12) shows the effect of loading ratio on  $(\alpha)$  profile for certain values of Reynolds number ( $Re=34006$ ) and particle size (300-425  $\mu m$ ). In general, as loading ratio increases  $(\alpha)$  decreases in the entrance of the pipe and increases at the end of test section. This means that the phase volume fraction is sensitive to increasing of loading ratio and so the gradient  $(\frac{\partial \alpha}{\partial x})$  which increases as the loading ratio increases. Fig.(13) shows the effect of Reynolds number on  $(\alpha)$  profile for loading ratio ( $L_R= 6$ ) and particle size (425-600  $\mu m$ ). The results show that as Reynolds number increases  $(\alpha)$  almost has the same profiles. The effect of loading ratio on velocity profiles are shown in fig.(14). The results show that, for certain values of Reynolds number ( $Re=34006$ ) and particle size (300-425  $\mu m$ ), as loading ratio increases the velocity increases along the pipe. This increase of the velocity may be caused by the decreasing in area occupied by the solid particles. Figure(15) shows how the velocity profile is influenced by the increasing of Reynolds number for a specific value of loading ratio (6) and particle size (425-600  $\mu m$ ). The increase in

---

velocities along the test section is due to the decreasing in gas density according to ideal gas assumption for the air. Figs (16) and (17) show the effect of the loading ratio and Reynolds number on the pressure profiles. As in the experimental results the pressures always increases as both Reynolds number and the loading ratio increase. Theoretically, we did not taken into account the effect the particle size in the modeling of the two phase flow. Even though, it is found that the experimental effect of particle size on the pressure profiles exists in theoretical results. This is because of the accurate prediction of this effect by the semi-empirical interaction parameter ( $S_a$ ). However, the pressures decrease as the particle size increases for almost the same values of loading ratio and Reynolds number.

## CONCLUSIONS

The following conclusions have been extracted from those experiments and the theoretical analysis:

1. The pressure gradient is strongly affected by Reynolds number rather than both loading ratio and particle size.
2. The pressure drops along the test section increase as Reynolds number and loading ratio increase and decreases as particle size increases.
3. The empirical correlation predicted in this work shows that the volume fraction ( $\alpha$ ) is the most affected parameter than Reynolds number and Froude number.
4. The theoretical analysis shows that the evaluations of pressure, pressure drop and friction coefficient, within the approximations in the model, are acceptable.
5. The theoretical pressure profile is always higher than experimental one.
6. The average difference between the theoretical friction coefficient and experimental is about ( 20 %).
7. The interaction (solid-gas) ,dimensionless number, ( $S_R$ ) is mainly affected by volume fraction ( $\alpha$ ).

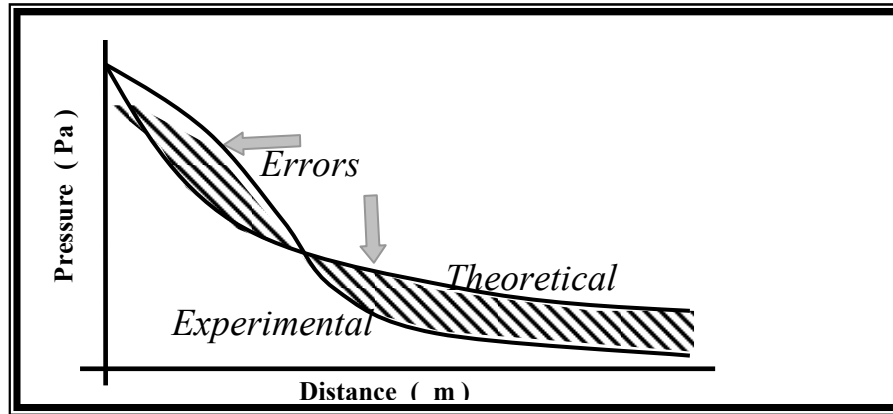


Fig.( 1 ): Objective function for minimizing errors of Eq. (7)

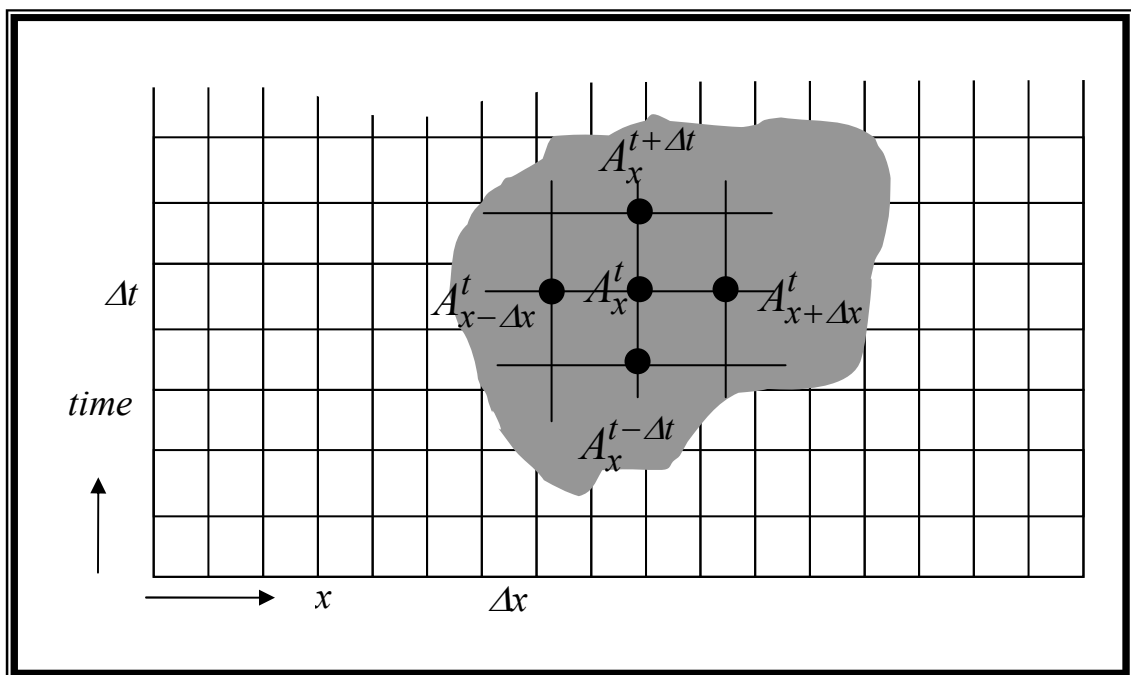
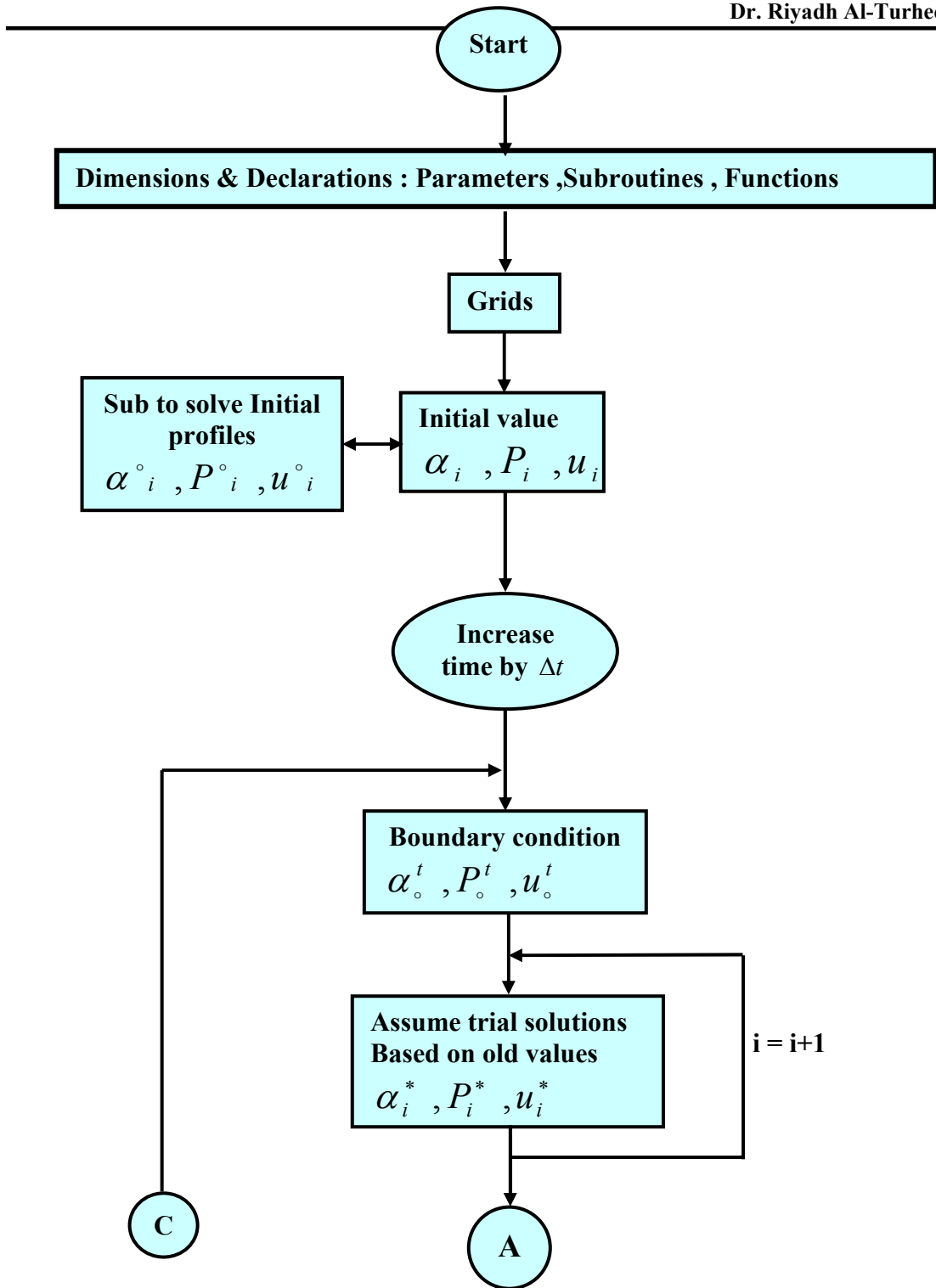


Fig.( 2 ): Regular grids in time-distance domains



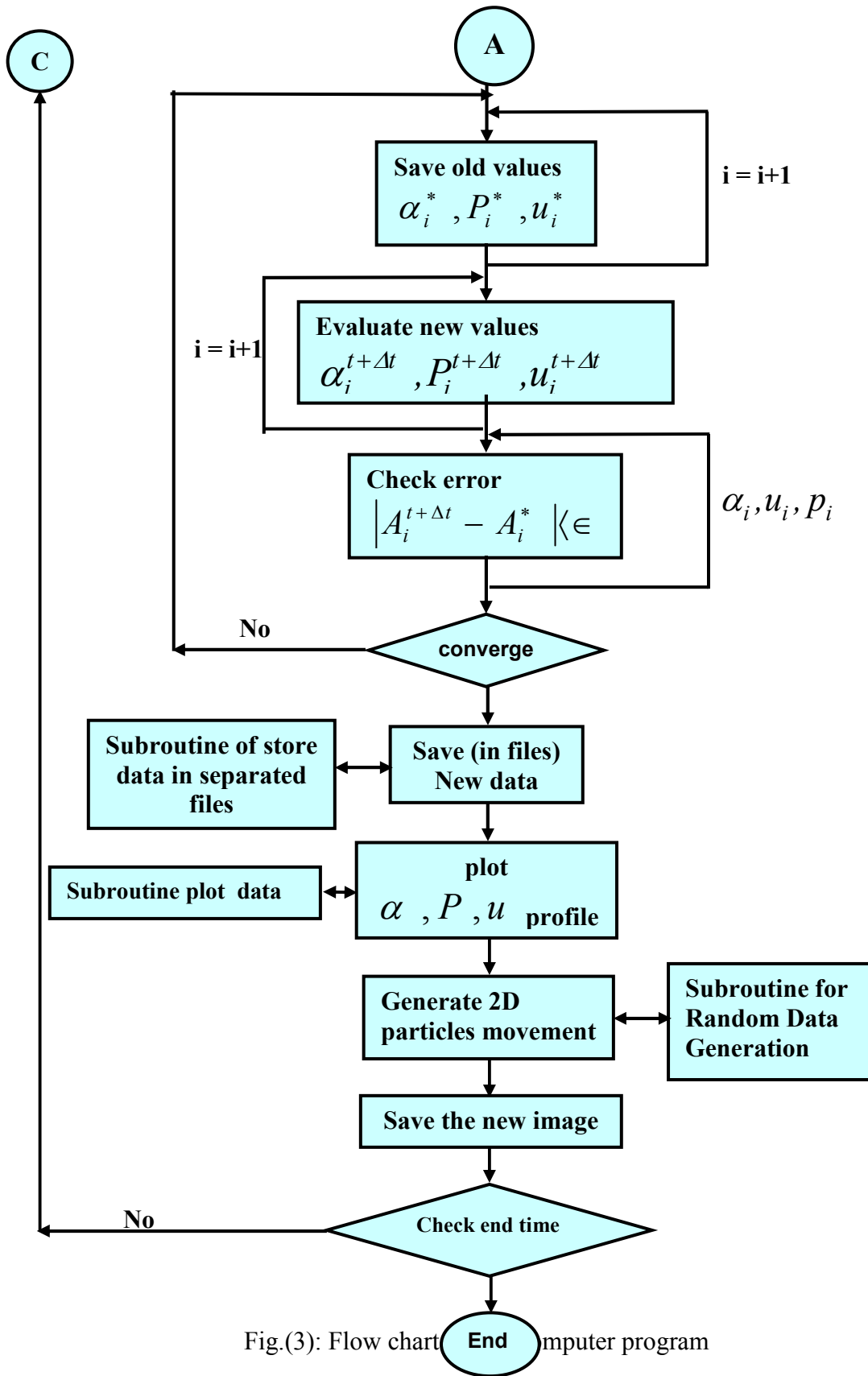


Fig.(3): Flow chart computer program

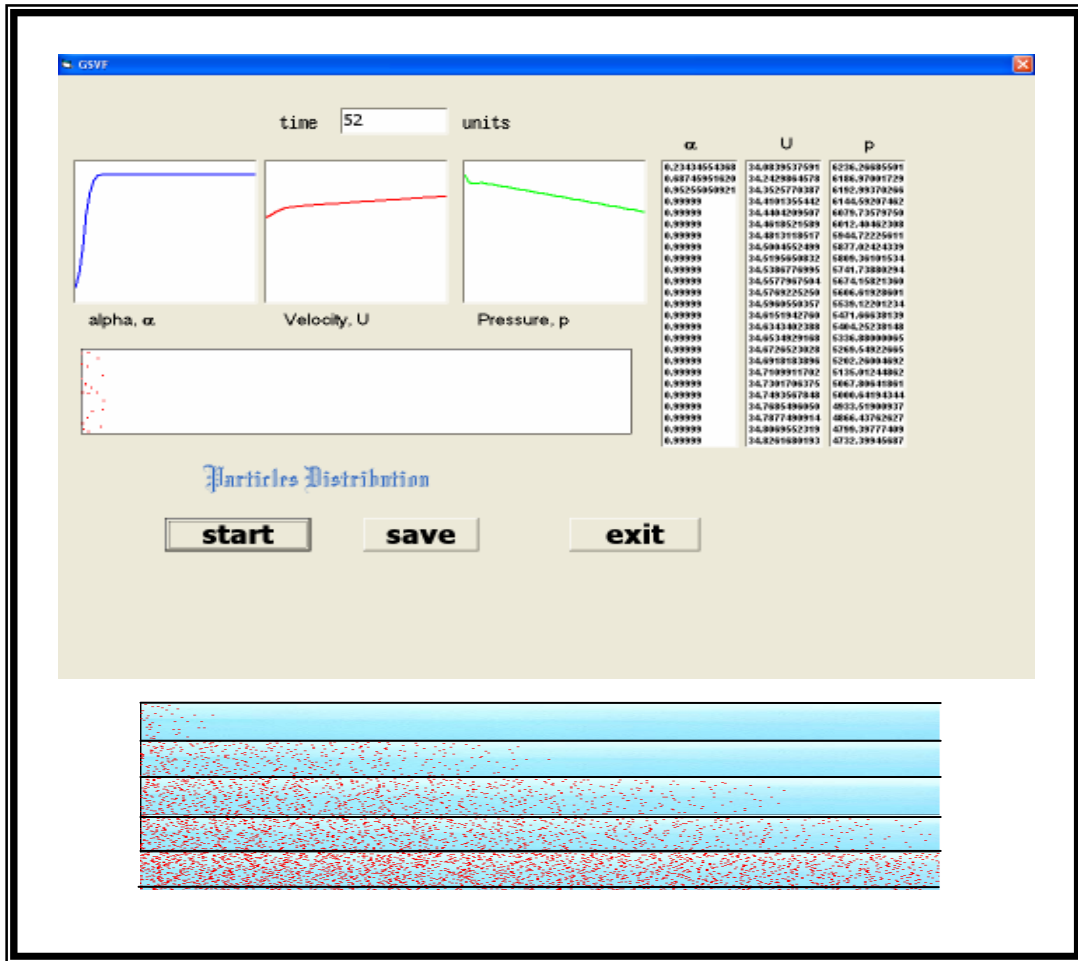


Fig.(4): Screen shot of GSVF with sample of images generated from the program.

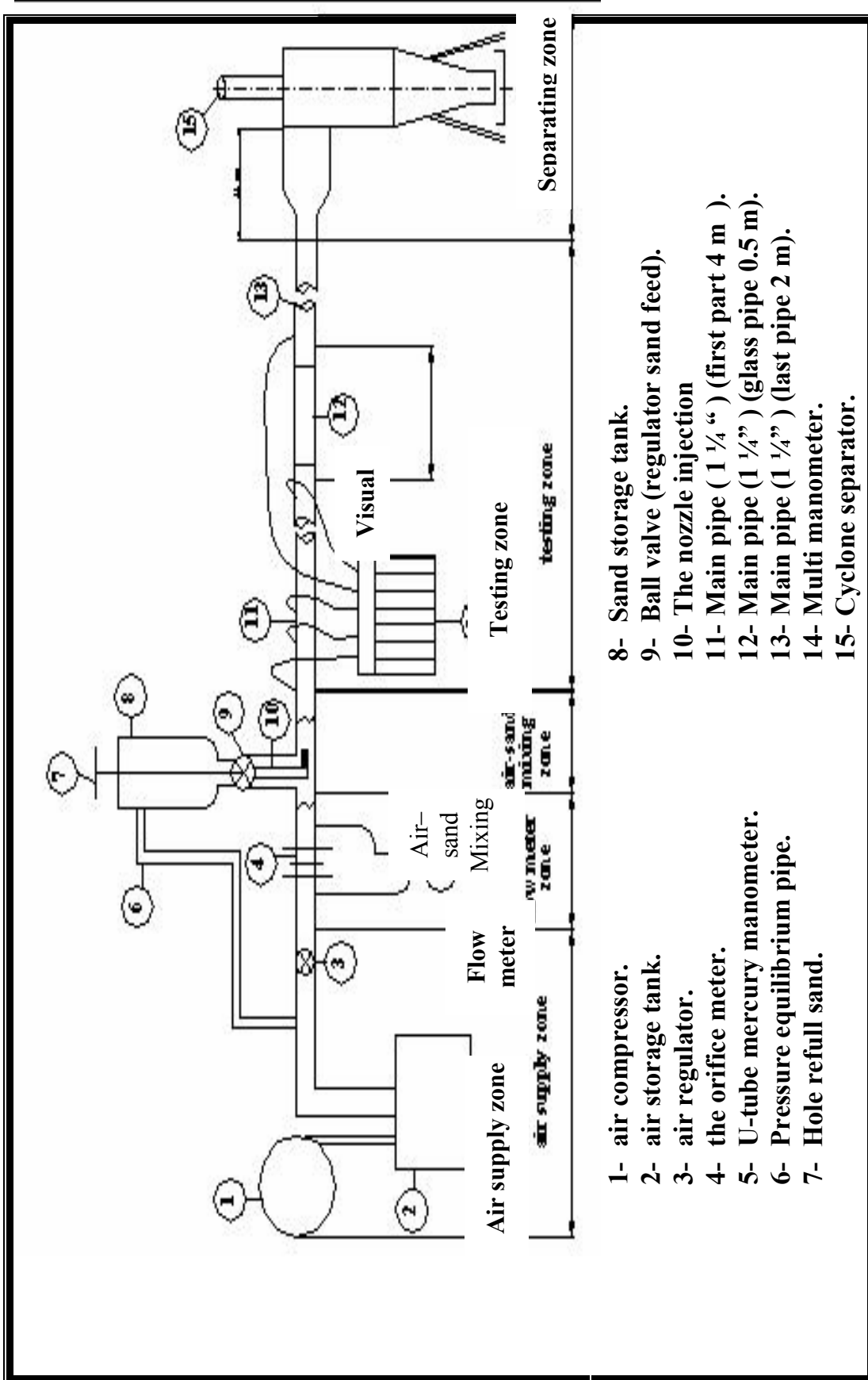


Fig. (5): the experimental equipments and measurement system

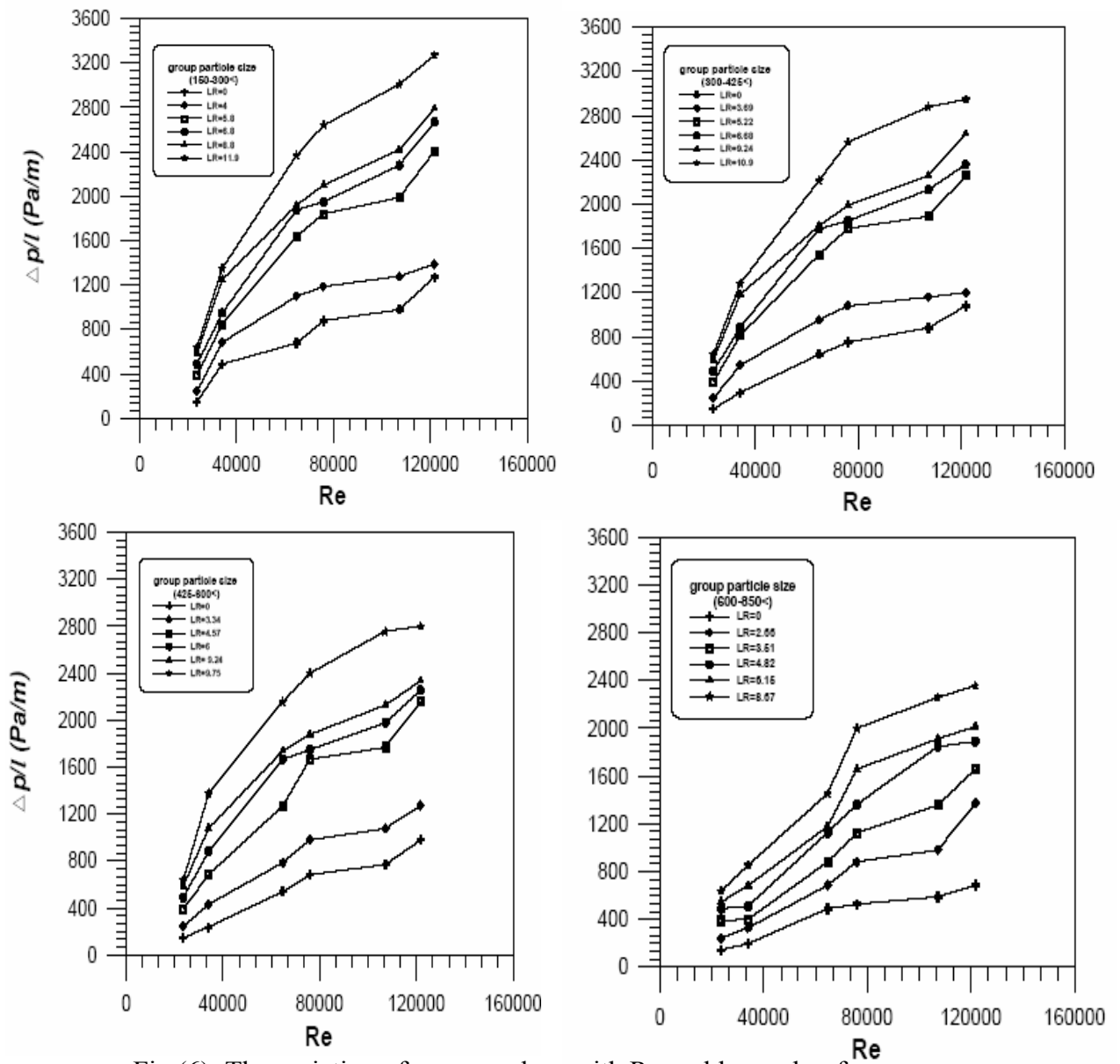


Fig.(6): The variation of pressure drop with Reynolds number for different particle size at different loading ratio

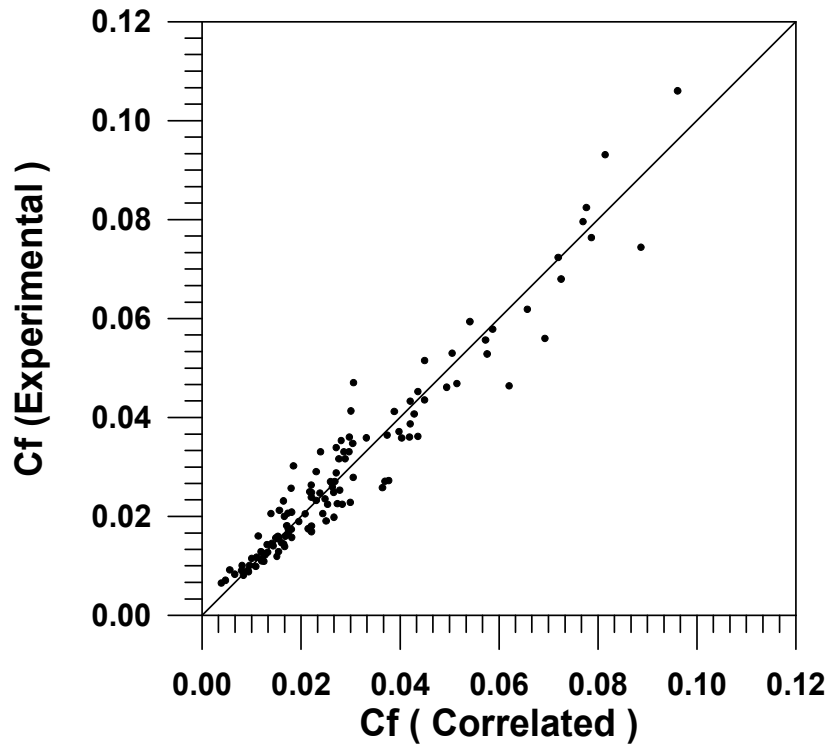


Fig.(7): A comparison between the experimental and the correlated friction coefficients eq. (5)

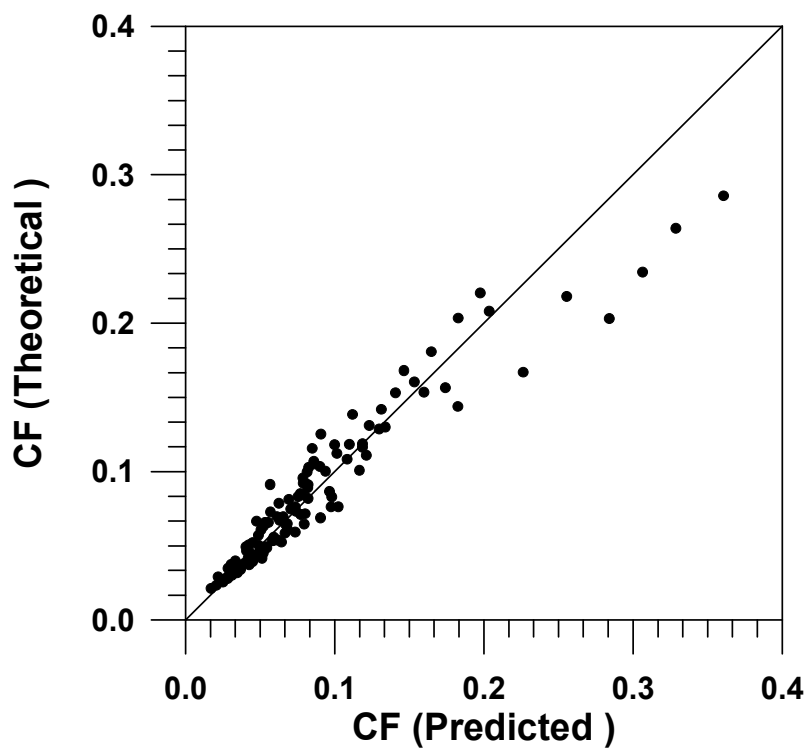


Fig.(8): A comparison between the theoretical and the correlated friction coefficients eq. (9)

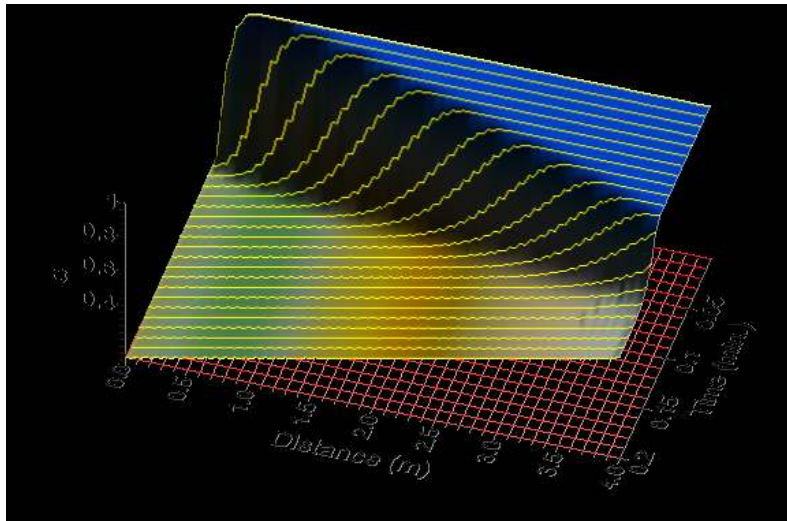


Fig.(9): A typical simulated transient behavior of volume fraction ( $\alpha$ ).

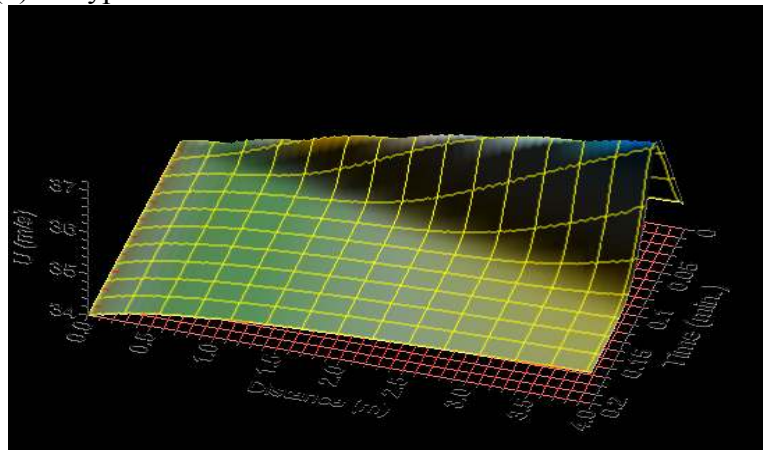


Fig.(10): A typical simulated transient behavior of velocity ( $U$ ).

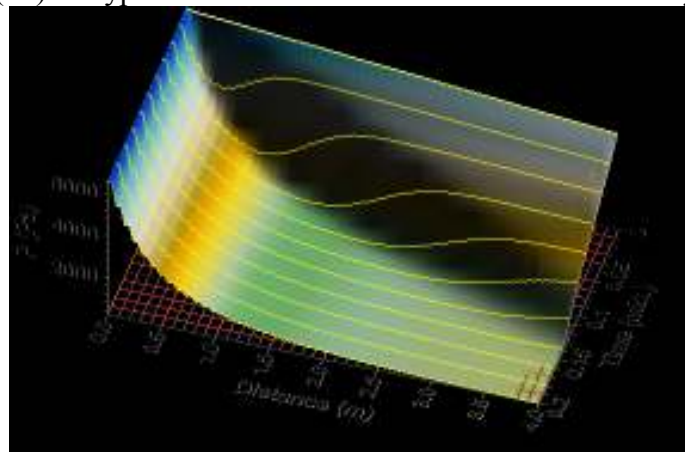


Fig.(11): A typical simulated transient behavior of pressure ( $p$ ).

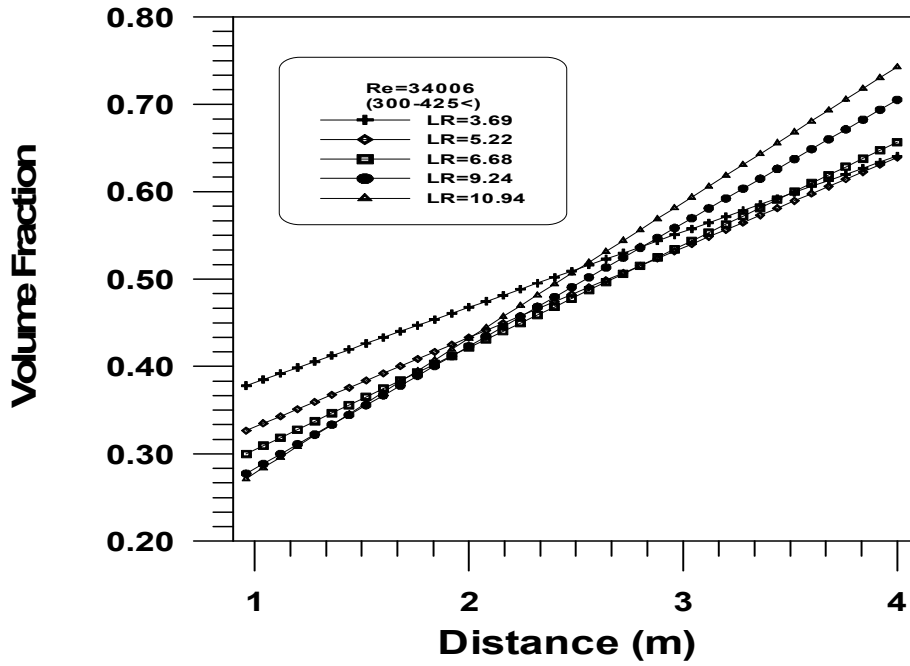


Fig.(12): Effect of Loading ratio on theoretical volume fraction profile

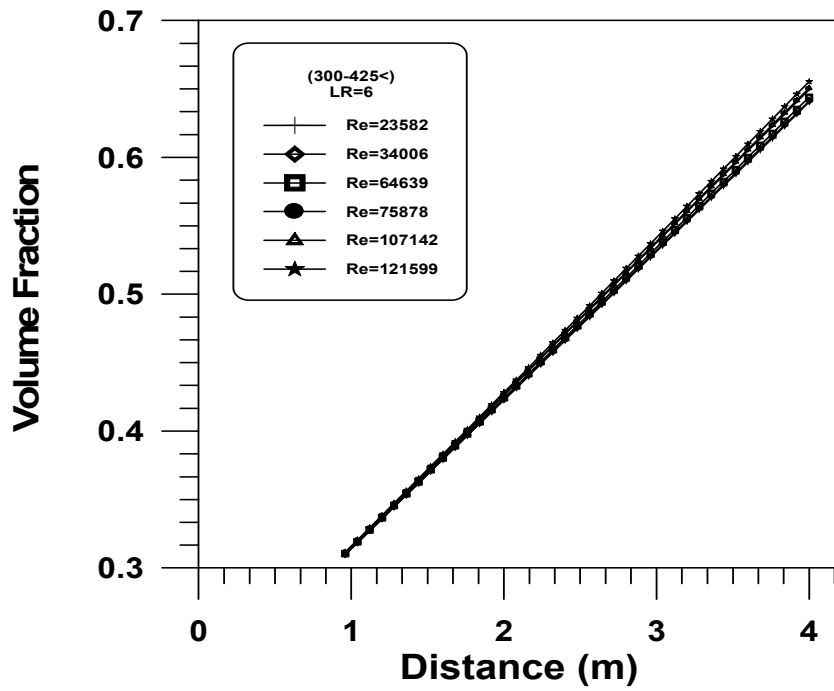


Fig.(13): Effect of Reynolds number on theoretical volume fraction profile

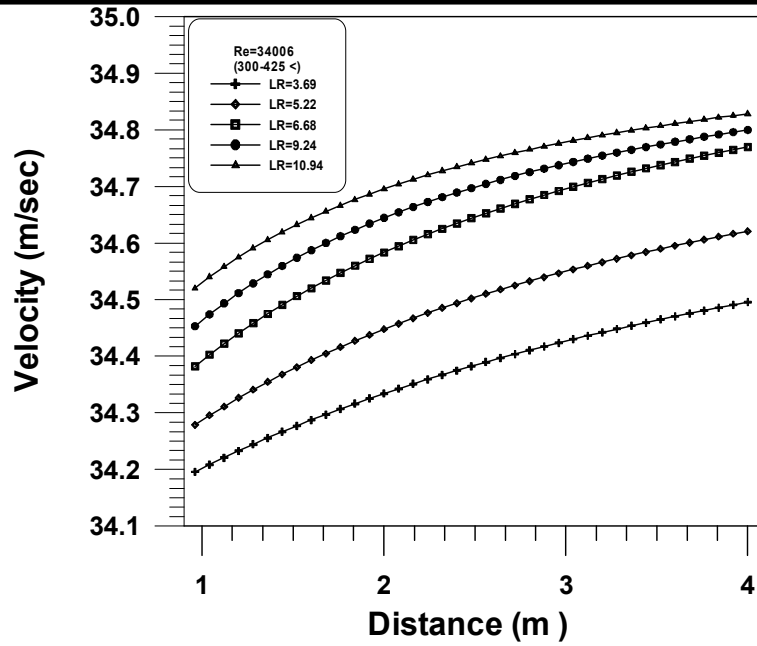


Fig.(14): Effect of loading ratio on theoretical velocity profile

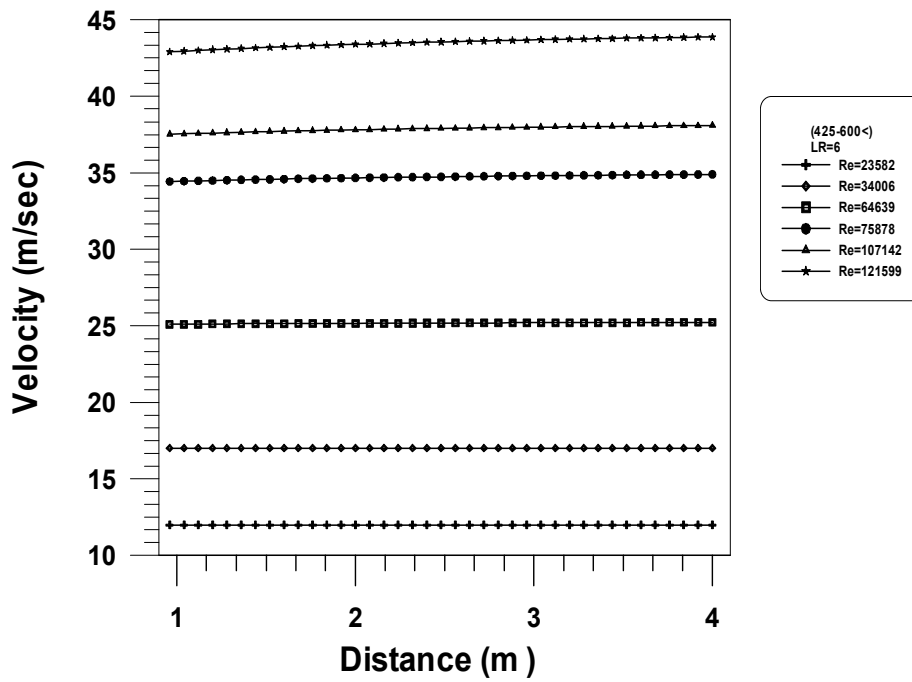


Fig.(15): Effect of Reynolds number on theoretical velocity profile

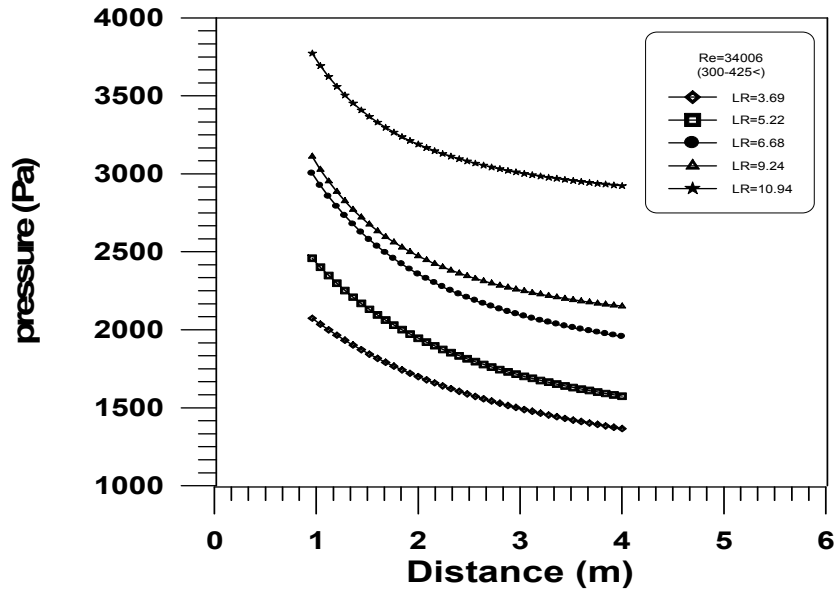


Fig.(16): Effect of loading ratio on theoretical pressure profile

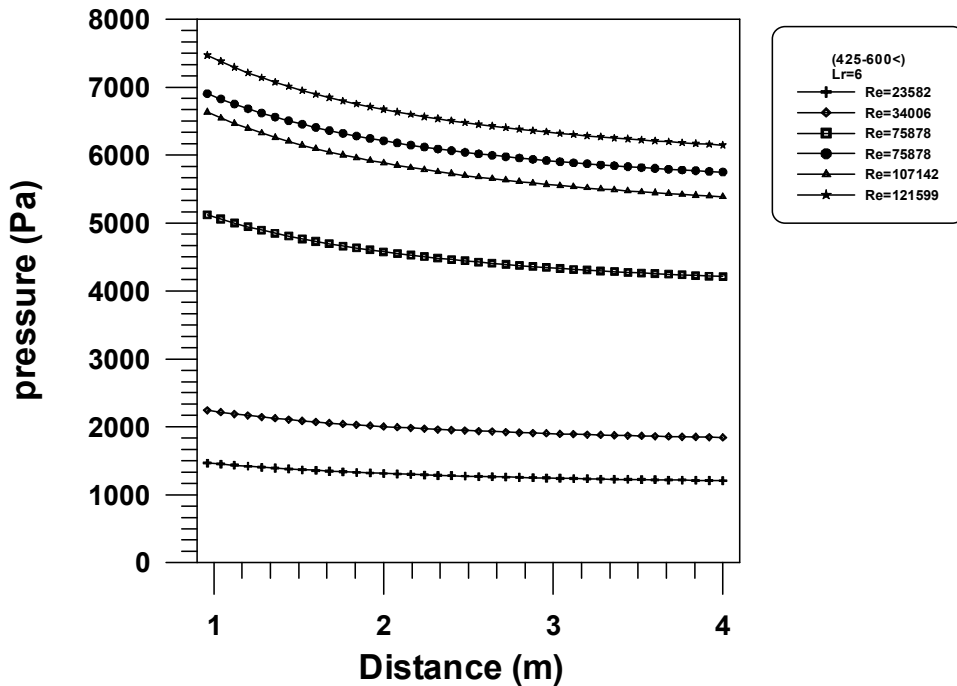


Fig.(17): Effect of Reynolds number on theoretical pressure profile

#### REFERENCE

A. Hamed And A. Mohamed, " Simultaneous Ldv Measvremnts Of Gas And Particle Velocities In Two-Phase Flow ", Proceedings Of Icfdp7: Seventh International Congress On Fluid Dynamic And Propulsion, Cairo, Egypt, December 19-21,2001.

A. Shimizu, R. Echigo And S. Hasegawa, " Experimental Study On The Pressure Drop And The Entry Length Of The Gas-Solid Suspension Flow In Circular Tube ", Int. J. Multiphase Flow, Vol. 4 , Pp. 53-64,1978.

---

Carpinlioglu And Gundogdu," Effect Of Particle Size And Loading On Development Region In Two-Phase Flow ", Tr. J. Of Engineering And Environmental Science 23 , Pp. 27-37,1999.

Denis Blackmore, Roman Samulyak And Anthouy Rosato, " New Mathematical Models For Particle Flow Dynamics ", Journal Of Nonlinear Mathematical Physics, Vol. 6 , No. 2, Pp. 198-221 , 1999.

G.A.Irons And J. S. Chang, " Particle Fraction And Velocity Measurement In Gas-Powder Streams By Capacitance Transducers", Int. J. Multiphase Flow Vol. 9 , No. 3 ,Pp. 289-297, 1983.

Kaoru Lwamoto, Koji Fukagata, Nabuhide Kasugi And Yuji Suzuki," Friction Drag Reduction Achievable By Near-Wall Turbulence Manipulation At High Reynolds Number ", Physics Of Fluids 17 , 011702 , 2005.

M. P. Sharam And C. T. Crowe, " A Novel Physico-Computational Model For Quasi One-Dimensional Gas-Particle Flow ", Journal Of Fluids Engineering Vol. 100 , Pp. 343-349 , September 1978.

M. Sommer Feld, S.Lain And J. Kussin, " Analysis Of Transport Effects Of Turbulent Gas-Particle Flow In Horizontal Channel " Proceedings 4<sup>th</sup> International Conference On Multiphase Flow, New Orleans, Icmf 2001.

Myung Kyoon Chung, Hyung Jin Sung And Kye Bock Lee," Computational Study Of Turbulent Gas-Particle Flow In Venturi ", Journal Of Fluids Engineering, Vol. 108 , Pp. 248-253 , June 1986.

Nikolai Andrianov, " Analytical And Numerical Investigation Of Two-Phase Flow ", Ph. D Thesis, Dtto-Von. Genericke University Magdeburg, 2003.

S. Benyahia, H. Arastoonpour, T. M. Knowlton And H. Massah," Simulation Of Particles And Gas Flow Behavior In The Riser Section Of A Circulating Fluidized Bed Using The Kinetic Theory Approach For The Particulate Phase ", E-Mail : Hamid. Arastoopour@lit.Edu , 2006.

S. Ni B. T. Chao And S. L. Soo," Particle Diffusivity In Fully Developed, Turbulent, Horizontal Pipe Flow Of Dilute Air-Solid Suspensions ", Int. J. Multiphase Flow Vol. 16 , No. 1, Pp. 43-56, 1990.

Tahssen A. Al-Hattab," Introduction In Numerical Methods ", First Edition, Handbook , 2005.

Vijay Kumar Stokes, " On The Flow Regimes Of Downhole Flow Of A Gas-Particle Mixture ", Asme Vol. 100, Pp. 410-412 , December 1978.

Y.Morika Wa, T. Kondo And Hiramoto, " Pressure Drop And Solids Distribution Of Air-Solids Mixture In Horizontal Unsymmetric Branches ", Int. J. Multiphase Flow, Vol. 4 , Pp. 397-404 , 1978.

Y. Tsuji, Y. Morikawa, T. Tanaka, N. Nakatsukasa And M. Nakatani," Numerical Simulation Of Gas-Solid Two Phase Flow In A Two-Dimensional Horizontal Channel ", Int. J. Multiphase Flow Vol. 13 , No. 5, Pp. 671-684, 1987.

Yang Ning, Wei Wang, Wei Ge, Jinghai Li, " Cfd Simulation Of Concurrent-Up Gas-Solid Flow In Circulating Fluidized Beds With Structure-Dependent Drag Coefficient ", Chemical Engineering Journal 96, Pp. 71-80, 2003.

Yutaka Tsuji And Yoshinobu Morikawa, " Flow Pattern And Pressure Fluctuation In Air-Solid Two-Phase Flow In A Pipe At Low Air Velocities ", Int. J. Multiphase Flow, Vol. 8 , Pp. 392-341 , 1982.

Yutaka Tsuji And Yoshinobu Morikawa, " Plug Conveying Of Coarse Particles In A Horizontal Pipe With Secondary Air Injection ", Int. J. Multiphase Flow, Vol. 8 , No. 6, Pp.657-667, 1982.

#### NOMENCLATURE

Symbol	Description	Symbol	Description
$A$	Area of orifice $m^2$	$m_s$	Mass flow of solid kg/s
$C_D$	Discharge coefficient	$m_a$	Mass flow of air kg/s
$C_f$	Friction coefficient $C_f = \frac{\Delta p}{\left(\frac{L}{D}\right)\rho_a\left(\frac{U^2}{2}\right)}$	$Q$	Air volumetric flow rate $m^3/s$
$C_p$	Specific heat at constant pressure KJ/kg.K	$P$	pressure $N/m^2$
$D$	Pipe diameter m	$Re$	Reynolds number $\frac{\rho U D}{\mu}$
$d_p$	Diameter of solid particle m	$R$	Gas constant =287 kJ/kg.K
$Fr$	Froude number $\left(\frac{U}{\sqrt{gd_p}}\right)$	$St$	Strouhal number
$g$	The acceleration due to gravity $m/s^2$	$Sa$	Interaction factor 1/s
$h$	Head of mercury manometer m	$S_R$	Suggested dimensionless number
$h_w$	Water head m	$T$	Temperature K
$L$	Length of test section m	$t$	Time s

$L_R$	Loading ratio	U	Velocity m/s
m	Mass of solid particle kg	x	Axial distance m
<b>GREEK SYMBOLS</b>			
$\rho$	Density kg/ m <sup>3</sup>	$\alpha$	Volume fraction
$\mu$	Newtonian dynamic viscosity N.s/m <sup>2</sup>	$\lambda, \gamma, \mu$	Constant equation
		$\Delta$	The difference between two values
<b>Subscripts</b>			
1	Inlet	g	Gas
2	At orifice	p	particle
i	Node of element	s	Solid
a	air		